ISSN 1648-7788 / eISSN 1822-4180

VILNIUS TECH
Vilnius Gediminas Technical University

AVIATION

2025
Volume 29
Issue 2
Pages 71–81
https://doi.org/10.3846/aviation.2025.23587

BLADE ELEMENT – MOMENTUM AERODYNAMIC MODEL OF A HELICOPTER ROTOR OPERATING AT LOW-REYNOLDS NUMBERS IN GROUND EFFECT

Gabriel GEORGIEV

Department of Aeronautics, Technical University of Sofia, Sofia, Bulgaria

Article History:
- received 21 September 2024
- accepted 9 January 2025

Abstract. The general objective of this paper is to present the initial results obtained as an outcome of applying a coupled Experimentally Derived – Blade Element Momentum Theory (BEMT) model for evaluating the airflow-defining parameters of a hovering helicopter rotor close to obstacles and making performance predictions. Several empirical models are described, and proper comparison with the experimentally obtained data is conducted. In detail, the characterization of the rotor inflow ratio (λ), when operating at fixed rotational frequency (n), at different relative distances to the ground (H/R), varying the pitching angle (θ) is discussed. The dependencies show an increase in the rotor inflow ratio parameter (λ), when increasing the collective pitch angle (θ) in hovering regime at fixed constant relative distance to the ground surface (H/R). On the contrary, the inflow ratio (λ) is experiencing a decline once the helicopter rotor operates closer to the ground surface. Moreover, the inflow ratio characterization (λ) along the blade span can be applied to the total generated thrust (T). As a result, the corresponding thrust coefficients (C_T) are calculated and graphically represented. The overall characterization of the thrust coefficients (C_T) will allow the definition of the ground effect zone.

Keywords: Blade Element – Momentum Theory, helicopter rotor, ground effect, rotorcraft aerodynamic characteristics, helicopter rotor flow characterization, helicopter rotor in hover.

Corresponding author. E-mail: *gabgeorgiev@tu-sofia.bg*

1. Introduction

Researching helicopter rotor performance during lifting off and landing has been an intriguing topic since the beginning of the extensive technical application and usage of rotary-wing machines. Performing aerodynamic performance prediction in different regimes and especially during lifting off is important for properly controlling the rotorcraft. Motivated by the Sikorsky human-powered helicopter competition, Gilad, Chopra, and Rand performed a study aimed to quantify the effect of the ground surface on the hovering rotor both experimentally and numerically (Gilad et al., 2011). The correlations between the coefficients of thrust (C_T) and power (C_P), varying the rotational frequency (n) have been numerically validated via rigid prescribed wake, blade element aerodynamic model, and finite-element structural model coupled together (Gilad et al., 2011). In detail, Nagaraj et al. (2021) introduced the design scheme and the aerodynamics characteristics of Gamera – the human powered helicopter. Full characterization of the rotor performance in ground effect conditions is presented both numerically and experimentally, including the derivation of the required power (Nagaraj et al., 2021). Free wake analysis via CAMRADII is being applied to study helicopter rotor behavior in Martian conditions by Koning et al. (2019). The Martian atmosphere is accountable for the reduction in the lift force and the efficiency of relatively small rotors operating at low Reynolds numbers. Graphical representation of the figure of merit and dependencies between the coefficients of power (C_P) and the coefficients of thrust (C_T) are derived and compared with experimentally obtained data (Koning et al., 2019).

In addition, Griffiths et al. (2005) introduced a free-vortex wake model based on the methods of images and surface singularity method for making airscrew performance predictions in ground effect, both in hover and in forward flight. The free-vortex prescription confirms the experimental trends for the rotor performance in the ground effect zone as a function of the ground proximity and the forward speed (Griffiths et al., 2005). As an outcome of the observed differences between the relaxation and time-marching free vortex wake results, the authors concluded that the flow in the ground effect zone is aperiodic (Griffiths et al., 2005). A computational model, suited to take into consideration the vortical structures in the rotor wake, which require many revolutions to develop, is applied by Brown and Whitehouse. The applied computational model confirms the experimental measurements and clearly illustrates that the helicopter rotor flow in ground effect undergoes different flow states as the helicopter rotor forward

speed increases (Brown & Whitehouse, 2004). The other flow states are represented through a connective instability of the vortex sheet, generated on the ground plane, providing an essential understanding of the rotor thrust and power characteristics (Brown & Whitehouse, 2004). Moreover, Khromov and Rand (2008) presented rotor wake modelling in and out of the ground effect zone for forward and axial flight. The proposed methodology includes rotor upwash modelling in the rotational plane and allows the determination of the helicopter rotor flight dynamics characteristics in both conditions (Khromov & Rand, 2008).

An experimental study of UAV propeller performance close to obstacles has been conducted by Georgiev et al. (2022). Presented dependencies quantify the correlation between the generated thrust (T) and power required (P) in the ground effect zone. Researchers observed an increase in the generated thrust (T) and a decline in the required power (P) once the propeller operates close to obstacles (Georgiev et al., 2022). The ground effect zone, where additional control actions might be required to ensure a safe landing, has been quantified.

Additionally, Georgiev et al. (2024) evaluated a helicopter rotor performance in ground effect taking into consideration several variable parameters such as the collective pitch angle (θ) and the relative distance to the ground (H⁄R) (Georgiev et al., 2024). Researchers showed experimentally obtained general dependencies regarding the rotor performance in hovering regime, including the generated thrust (T) vs. the rotational frequency (n) at fixed collective pitch angle (θ), varying the relative distance to the ground (H⁄R), and the torque required (Q) vs. the rotational frequency (n) for different relative distances to the ground (H⁄R) at a fixed collective pitch angle (θ). The corresponding coefficients have been evaluated and their dependencies have been depicted, (C_T) and (C_Q), respectively (Georgiev et al., 2022). Moreover, the ground effect zone has been characterized.

Wind tunnel measurements below and ahead of the helicopter's main rotor in forward flight have been presented by Nathan and Green. The wind tunnel equipment includes a moving ground surface for the representation of the forward flight over the ground (Nathan & Green, 2011). A study of the flow structures has been performed using a particle image velocimetry and a reduction in the wake is observed when including the moving ground surface (Nathan & Green, 2011). Investigation of helicopter rotor handling qualities in ground effect has been conducted by Hanker and Smith. Changes in helicopter forces and moments have been observed because of the changes in the main rotor thrust (Hanker & Smith, 1985). Moreover, an experimental study regarding the helicopter rotor flow field in ground effect is presented by Kutz et al. (2013) The wake trajectory has been obtained by introducing fog in the rotor disk for the sake of flow visualization by applying laser light and a high-speed camera (Kutz et al., 2013).

A description of helicopter aerodynamics in ground effect, presented in terms of performance effects is conducted by Fradenburgh. An increase in thrust force (T) values when the rotor operates in the ground effect zone is presented and no additional power required (P) in the transitional mode from hover in ground effect to forward flight is characterized, as well (Fradenburgh, 1960). Eberhart and Wilhelm (2018) presented a coupled Empirical – BEMT code for a UAV propeller operating in ground effect. The code successfully predicts the thrust (T) and the coefficient of thrust (C_T), which is 33% higher in the ground effect zone (Eberhart & Wilhelm, 2018). A free wake model for predicting the hovering rotor performance in ground effect is recommended by Graber et al. (1991). As a result of its application, a good agreement for the coefficients of thrust (C_T), validated with existing experimental results, is achieved and discrepancies regarding the torque (Q) values are presented (Graber et al., 1991). Further analysis describes correlation functions, which relate both the parameters in and out of the ground effect zone (Johnson, 2019). These correlations include parameters, such as the inflow distribution ratio (λ), the rotor coefficient of thrust in the ground effect zone (C_T), the airscrew solidity (σ), and the relative distance to the ground surface (H⁄R) and can be directly applied for finding both the coefficients of thrust (C_T) and power (C_P) in the ground effect zone (Johnson, 2019). Some of the models describe the connection via applying the blade element theory, including Cheeseman and Bennett, while others use experimentally derived data for finding the correlation between the parameters in and out of the ground effect zone, such as the University of Maryland and Zbrozek models (Johnson, 2019). Implementation of the Cheeseman and Bennett model for validating experimental results in ground effect has been proposed by Conyers et al. (2018). A comparison between numerical and experimental results for several multirotor and single–rotor configurations has been presented (Conyers et al., 2018). Findings show that the conventional model cannot be directly applied to the helicopter rotor in ground effect for several specific cases and a proper correction must be applied.

Knight and Hefner presented a numerical study, aiming to quantify the effect on the thrust (T) and torque (Q) of an airscrew, operating in ground effect conditions, based on the reflection method. An increase in the thrust force (T) values is observed when the rotor operates at a distance lower than one diameter to the ground surface. Results show that the torque values (Q) remain relatively constant, except for the very low distances to the ground (Knight & Hefner, 1941). Calculation of induced power values, when a helicopter rotor operates near the ground surface is quantified through applying a modified actuator disk model (Lighthill, 1979). As a result, a decrease in the induced power values is observed in the ground effect zone in comparison with results for a rotor operating away from it.

Implementation of BEMT model for aerodynamic analysis of newly designed micro air vehicles is suggested by Bohorquez et al. (2023). Figures of merit, dependencies

between the power (C_P) and thrust (C_T) coefficients have been drawn. Comparisons, taking into consideration experimentally obtained data and the numerically derived through applying a BEMT model, are shown. The model predicts an increase of 15% in the losses due to profile drag in comparison with a full-scale helicopter (Bohorquez et al., 2023).

Blade element momentum model modifications, based on numerical and experimental results, have been proposed by Madsen et al. Deviations are observed both on the inner and the outer surface of the rotor model in comparison with other numerical simulations (Madsen et al., 2007). On the inner surface, the BEM model overestimates the induction by neglecting the pressure term from rotation, while on the outer surface, an underestimation is observed due to the expansion of the stream tubes (Madsen et al., 2007).

Pulla and Conlisk (2007) presented lifting surface theory and method of image algorithms coupled together for the sake of modelling the ground effect. Calculation of wake geometry for several forward flight speeds has been performed and compared with flow visualization techniques (Pulla & Conlisk, 2007) for analyzing the helicopter rotor handling qualities. The handling qualities are considered to depend on the presence or absence of large unsteady fluctuations in the rotor wake due to interference of the ground vortex with the helicopter rotor and the fuselage (Pulla & Conlisk, 2007). Helicopter rotor performance analysis in the ground effect zone, applying numerical, asymptotic, and flow structural techniques is presented by Purvis. The study includes analyzing different configurations including 3-D analysis to investigate the flow structures (Purvis, 2002). Application of a flow solver which combines both the viscous particle method with a viscous ground model is applied for investigating the rotor wake interaction in ground effect. Generally, the applied viscous particle method is based on the Navier – Stokes equations and the grid-free Lagrangian formulation. In contrast, the viscous ground model is implemented to satisfy the no-slip boundary condition in the viscous particle method (Zhao & He, 2015). The flow solver is directly implemented in simulations for the sake of studying the rotor tip vortex dynamics, ground vortex formation, rotor hover performance, forward flight, and rotor outwash calculations. Additionally, the authors investigated the effect of interference between the main and the tail rotors and the ground vortex on the tail rotor performance (Zhao & He, 2015).

Todorov et al. (2012) introduced a Blade Element Momentum model for aeroelastic studies of a helicopter rotor in hover. The aerodynamic model accounts for the evaluation of aerodynamic forces, while it is coupled with the Finite Element Model for aeroelastic predictions. Moreover, the model represents the lift (L) and drag (D) forces distribution along the blade radius (R), considering the balance between time and accuracy (Todorov et al., 2012). Rotaru and Todorov (2017) analyzed the effect on the helicopter rotor efficiency, when it operates in ground effect. The authors prescribed an increased efficiency due to the interference with the ground, and a rise in the L/D ratio (Rotaru & Todorov, 2017).

The general objective of this study is to quantify numerically the velocity distribution in the helicopter rotor plane of rotation for several operational cases when hovering in ground effect conditions. The research objective will be completed by empirically correcting the inflow ratio distribution (λ) for the rotor rotational plane in the applied Blade Element – Momentum model. Taking off and landing from fields with limited areas such as rooftop helipads or air carriers require detailed research regarding the aerodynamic characteristics in the ground effect zone. The numerical quantification of ground effect will provide essential operational information regarding the helicopter rotor performance during take-off and landing, applicable to the design of flight controllers.

Specifically, the research tasks include a preliminary evaluation of the rotor inflow ratio (λ), varying the pitch angle (θ) and the relative distance to the ground (H/R) via applying a coupled empirical-blade element-momentum algorithm. The first step requires evaluation of the inflow ratio (λ) outside the ground effect zone for the whole set of pitching angles $\theta_1 = 9°$, $\theta_2 = 12°$, $\theta_3 = 15°$, $\theta_4 = 18°$, $\theta_5 = 21°$. Afterwards, the thrust coefficients (C_T) can be directly evaluated, once the convergence tolerance has been achieved. Following the evaluation of the thrust coefficients (C_T) for the hovering rotor outside the ground effect zone, an empirical correction in the inflow ratio (λ) is applied to take into consideration the effect on the inflow ratio (λ), when the rotor operates close to the ground surface. As a result, a preliminary quantification of the inflow ratio (λ) and the normalized thrust coefficient (C_T/σ) varying the pitching angle (θ) and relative distance to the ground (H/R) are expected to be evaluated and compared with existing experimental data.

2. Blade Element Momentum Theory (BEMT) Model

The combination between the Blade Element and Momentum Theory allows the calculation of the inflow ratio distribution (λ). The inflow ratio distribution can be derived by considering the Blade Element and Momentum Theory expressions for the differential coefficients of thrust (C_T) in hover (Johnson, 2013).

The differential coefficient of thrust (C_T), derived by applying the Blade Element Theory, can be expressed by Equation (1) and Equation (2):

$$dC_T = dC_L \cos(\varphi) - dC_D \sin(\varphi); \quad (1)$$

$$dC_T = \frac{\sigma a}{2}\left(\theta - \frac{\lambda}{r}\right) r^2 dr, \quad (2)$$

where dC_L – denotes the blade element lift force coefficient, dC_D – blade element drag force coefficient, φ – in-

duced angle of attack, σ – designates the rotor solidity, *a* – blade section two-dimensional lift-curve slope, *r* – blade radial coordinate, θ – blade pitch angle of each section, $\lambda = \lambda_C + \lambda_i$ – inflow ratio, $\lambda_c = V/\Omega R$ – climb inflow ratio, $\lambda_i = \upsilon/\Omega R$ – induced inflow ratio, V: climb speed, υ – induced velocity (Leishman, 2006; Johnson, 2013).

Considering that the induced angles of attack (φ) remain relatively low, and the velocity vector $U \approx U_T$, the increment of the thrust coefficient (dC_T) is (3) (Leishman, 2006):

$$dC_T = \frac{dL}{\rho A(\Omega R)^2} = \frac{\left(\frac{1}{2}\rho U_T^2 c C_L dy\right)}{\rho(\pi R^2)(\Omega R^2)} = \frac{1}{2}\left(\frac{c}{\pi R}\right)C_L\left(\frac{y}{R}\right)^2 d\left(\frac{y}{R}\right) = \frac{1}{2}\frac{c}{\pi R}C_L r^2 dr, \quad (3)$$

where ρ – air density, *A* – rotor disk area, Ω – rotational frequency, *R* – rotor radius, *c* – blade element chord, U_T – in plane velocity component, *y* – blade element radial coordinate.

The differential form of the thrust coefficient (C_T), derived from the Momentum Theory, can be expressed via Equation (4):

$$dC_T = 4\lambda\lambda_i r dr\,. \quad (4)$$

Taking into consideration and equating both the Blade Element and Momentum Theory expressions for the (C_T) allows us to derive the following expression for the inflow distribution (λ) (Johnson, 2013):

$$\lambda^2 + \left(\frac{\sigma a}{8} - \lambda_c\right)\lambda - \frac{\sigma a}{8}\theta r = 0\,. \quad (5)$$

For the hovering regime ($\lambda_c = 0$) Equation (5) has the following solution (Equation (6)) (Johnson, 2013):

$$\lambda = \frac{\sigma a}{16}\left[\sqrt{1 + \frac{32}{\sigma a}\theta r} - 1\right]. \quad (6)$$

As a result, the coefficient of thrust (C_T) can be calculated by integrating the (dC_T) values along the blade radius (*r*) (Equation (7)):

$$C_T = \int_0^R dC_T\, dr\,. \quad (7)$$

Following the evaluation of the thrust coefficient (C_T), the differential power coefficient (C_P) can be estimated, according to Equations (8) and (9) (Johnson, 2013):

$$dC_P = \left[\lambda\frac{\sigma a}{2}\left(\theta r^2 - \lambda r\right) + \frac{\sigma C_d}{2}r^3\right]dr, \quad (8)$$

where C_d – the blade element drag force coefficient.

$$dC_P = \lambda dC_T + \frac{\sigma C_d}{2}r^3 dr\,. \quad (9)$$

The total power coefficient (C_P) can be evaluated by integrating the (dC_P) values along the blade span (Equation (10)):

$$C_P = \int_0^R dC_P\, dr\,. \quad (10)$$

3. Empirical models

Several empirical models have been developed by researchers for making predictions regarding the aerodynamic performance of rotors operating in ground effect conditions. Figure 1 represents empirical models, derived by different researchers, working in the field of helicopter rotor aerodynamics in ground effect. All the models represent the connection between the general aerodynamic parameters in and out of the ground effect zone, such as the thrust in and out-ground effect and the power required in both conditions. The data presented in Figure 1 (Johnson, 2019), illustrate the dependency between the relative thrust in and out of the ground effect zone (T/T_∞) and the relative distance to the ground surface (z/R). The curves thereby show that the ground effect zone covers the approximate lengths between the ground surface and the rotor plane of rotation equal to 2R.

The closer to the ground the rotor operates, the higher decrease in the inflow distribution is observed, and a corresponding increase in the amount of the generated thrust can be measured or computed. A shift in the magnitude of the thrust can be observed from the dependencies derived by different researchers. The shift in the data originates from the base of each one of the empirical models and the parameters that they take into consideration. The University of Maryland model includes the application of polynomial interpolation of experimentally measured data. Except for the University of Maryland, all the other models apply other type dependencies of different rank power, considering several parameters such as the rotor solidity (σ), the thrust coefficient (C_T), the lift force curve gradient (a), and the relative distance to the ground surface (z_g/R).

Empirical models are represented by means of the function (f_g). The function (f_g) expresses the correlation between the induced inflow ratio (λ_i) in the ground effect zone and out of it, and consequently the correlation between the thrust in both conditions, according to Equation (11) (Johnson, 2013):

$$\lambda_{iIGE} = f_g \lambda_{iOGE}. \quad (11)$$

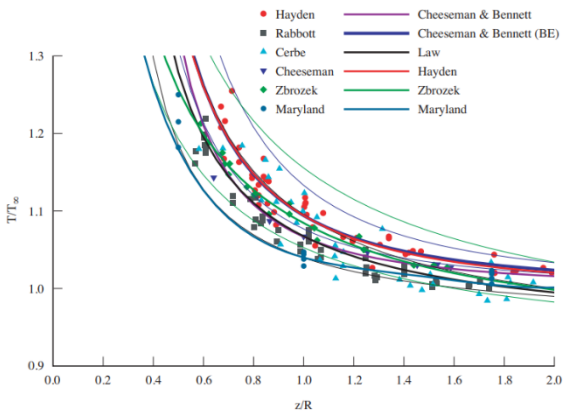

Figure 1. Relative Thrust (T/T∞) vs. Relative Distance to the Ground (z/R) according to different researchers (Johnson, 2013)

The Zbrozek model is represented with the function $f_{g_{Zbrozek}}$, expressed by Equation (12) (Johnson, 2013):

$$f_{g_{Zbrozek}} = \left[0.9122 + \frac{0.0544}{\left(z_g / R\right)\sqrt{C_T / \sigma}}\right]^{-3/2}. \quad (12)$$

The Hayden model includes the function $f_{g_{Hayden}}$, according to Equation (13) (Johnson, 2013):

$$f_{g_{Hayden}} = \left[0.9926 + \frac{0.03794}{(z_g / 2R)^2}\right]^{-1}. \quad (13)$$

The University of Maryland polynomial model is expressed via Equation (14) (Johnson, 2013):

$$f_{g_{UMD}} = 0.146 + 2.090\left(\frac{z_g}{R}\right) - 2.068\left(\frac{z_g}{R}\right)^2 + 0.932\left(\frac{z_g}{R}\right)^3 - 1.157\left(\frac{z_g}{R}\right)^4. \quad (14)$$

The Cheeseman and Bennett model can be derived via Equation (15), as follow (Johnson, 2013):

$$f_{g_{CB}} = [1 + 1.5\frac{\sigma a \lambda_i}{4C_T}\frac{1}{\left(4\frac{z_g}{R}\right)^2}]^{-3/2}. \quad (15)$$

In Tables 1, 2, 3 and 4 comparisons between the experimentally obtained data and results derived by applying the empirical models represented above are shown for the sake of finding empirical corrections, which will be applied to the Blade Element – Momentum Model. In the tables below relative thrust force coefficients in and out of the ground effect zone C_{TIGE} / C_{TOGE} obtained through the application of Zbrozek, Hayden, UMD and Cheeseman and Bennett models are illustrated along with the experimental results, varying the collective pitch angle (θ). Generally, the obtained results show that Hayden's model provides better coverage with the experimental C_{TIGE} / C_{TOGE} ratio for collective pitch angles θ < 18°, while in the high pitch angles (θ) region the model does not provide good coverage. Conversely, Cheeseman and

Table 1. Experimental and Zbrozek's model relative thrust force coefficients C_{TIGE} / C_{TOGE}, varying the rotor's collective pitch angle (θ) and the relative distance (H/R)

C_{TIGE} / C_{TOGE} Experimental and Empirical results by applying the Zbrozek model								
H/R	θ_1 = 9°		θ_2 = 12°		θ_4 = 18°		θ_5 = 21°	
	EXPT	EMP	EXPT	EMP	EXPT	EMP	EXPT	EMP
2	1.00	1.65	1.00	1.50	1.00	1.40	1.00	1.35
1	1.25	2.25	1.18	1.90	1.20	1.75	1.17	1.65
0.5	1.75	3.20	1.40	2.80	1.25	2.40	1.21	2.40
0.25	2.10	5.10	1.70	4.40	1.20	4.00	1.18	3.90

Table 2. Experimental and Hayden's model relative thrust force coefficients C_{TIGE} / C_{TOGE}, varying the rotor's collective pitch angle (θ) and the relative distance (H/R)

C_{TIGE} / C_{TOGE} Experimental and Empirical results by applying the Hayden model								
H/R	θ_1 = 9°		θ_2 = 12°		θ_4 = 18°		θ_5 = 21°	
	EXPT	EMP	EXPT	EMP	EXPT	EMP	EXPT	EMP
2	1.00	1.00	1.00	1.00	1.00	1.00	1.00	1.00
1	1.25	1.15	1.18	1.14	1.20	1.13	1.17	1.13
0.5	1.75	1.44	1.40	1.41	1.25	1.36	1.21	1.35
0.25	2.10	2.26	1.70	2.25	1.20	2.25	1.18	2.30

Table 3. Experimental and UMD's model relative thrust force coefficients C_{TIGE} / C_{TOGE}, varying the rotor's collective pitch angle (θ) and the relative distance (H/R)

C_{TIGE} / C_{TOGE} Experimental and Empirical results by applying the UMD model								
H/R	θ_1 = 9°		θ_2 = 12°		θ_4 = 18°		θ_5 = 21°	
	EXPT	EMP	EXPT	EMP	EXPT	EMP	EXPT	EMP
2	1.00	1.00	1.00	1.00	1.00	1.00	1.00	1.00
1	1.25	1.00	1.18	1.00	1.20	1.00	1.17	1.00
0.5	1.75	1.00	1.40	1.10	1.25	1.05	1.21	1.03
0.25	2.10	1.25	1.70	1.45	1.20	1.40	1.18	1.38

Table 4. Experimental and Cheeseman and Bennett's model relative thrust force coefficients C_{TIGE} / C_{TOGE}, varying the rotor's collective pitch angle (θ) and the relative distance (H/R)

(C_{TIGE} / C_{TOGE}) Experimental and Empirical results by applying the Cheeseman and Bennett model								
H/R	θ_1 = 9°		θ_2 = 12°		θ_4 = 18°		θ_5 = 21°	
	EXPT	EMP	EXPT	EMP	EXPT	EMP	EXPT	EMP
2	1.00	1.00	1.00	1.00	1.00	1.00	1.00	1.00
1	1.25	1.10	1.18	1.10	1.20	1.08	1.17	1.07
0.5	1.75	1.20	1.40	1.12	1.25	1.10	1.21	1.10
0.25	2.10	1.25	1.70	1.18	1.20	1.24	1.18	1.22

Bennett's model fits better to the experimental results in the high pitch angles region (θ > 18°) and does not provide good coverage in the low pitch angles zone (θ < 18°).

Figure 2a, 2b and Figure 3a, 3b represent the dependencies between the relative thrust coefficients in and out-ground effect zone ($C_{T_{IGE}}/C_{T_{OGE}}$) and the relative distances to the ground (H/R) as an outcome of applying some of the empirical models and part of the experimental results measured at rotational frequency n = 950 rpm varying the pitching angles as follows θ_1 = 9°, θ_2 = 12°, θ_4 = 18° and θ_5 = 21°, according the results presented in Tables above.

According to the presented correlations it can be concluded that the Hayden empirical model can be applied for correcting the inflow for small pitching angles to up to θ_4 = 18°, while the Cheeseman and Bennett model provides better coverage of the experimental curves for pitching angles θ_4 > 18° in extreme ground effect conditions.

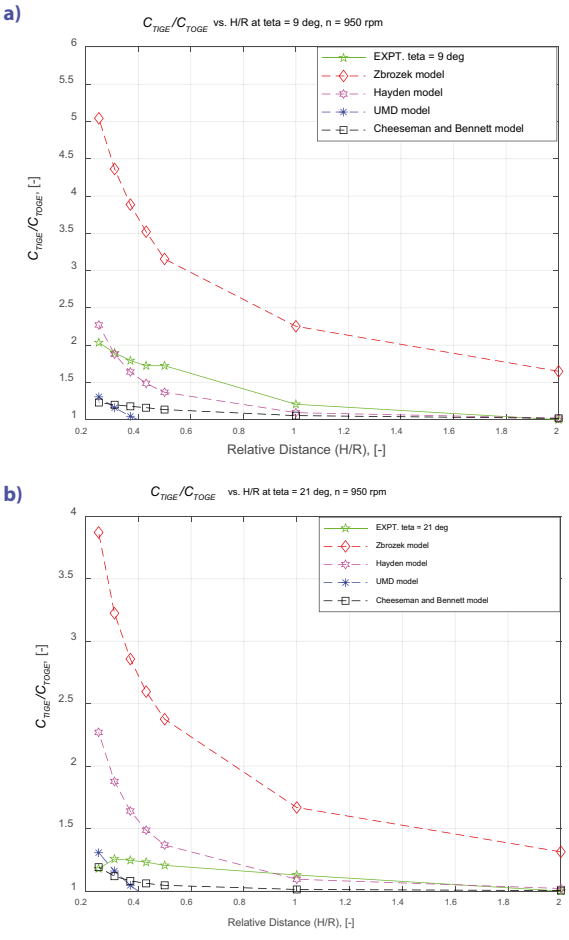

Figure 2. Relative thrust coefficient ($C_{T_{IGE}}/C_{T_{IGE}}$) vs. relative distance to the ground (H/R) experimentally derived and empirically evaluated: a – pitch angle θ_1 = 9°; b – pitch angle θ_2 = 12°

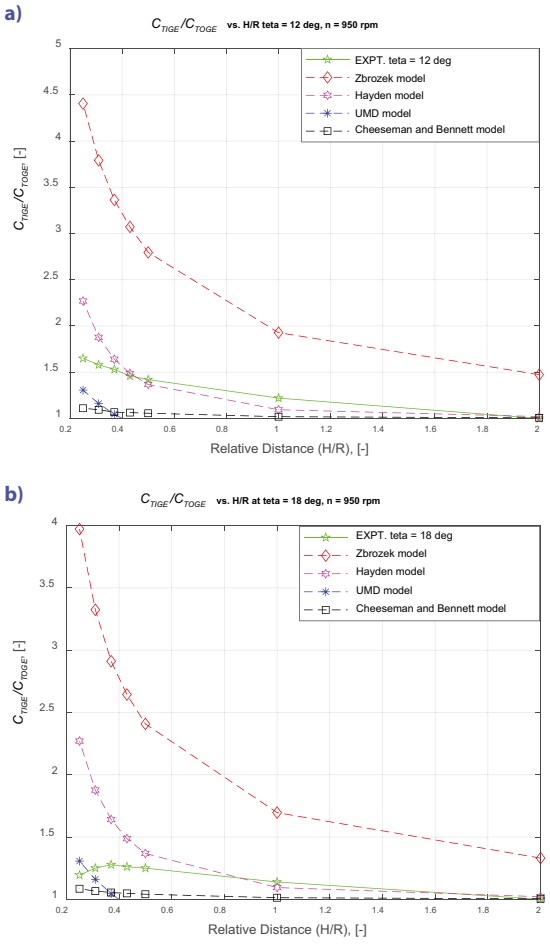

Figure 3. Relative thrust coefficient ($C_{T_{IGE}}/C_{T_{IGE}}$) vs. relative distance to the ground (H/R) experimentally derived and empirically evaluated: a – pitch angle θ_4 = 18°; b – pitch angle θ_5 = 21°

In this computational case, the Hayden model is being applied for correcting the inflow distribution (λ) for the pitching angles $\theta_4 < 18°$, while the Cheeseman and Bennett model is applied for correcting the inflow distribution for pitching angles $\theta_4 > 18°$ in extreme ground effect.

4. Calculation methodology

The calculation methodology includes several steps required for the computation of rotor inflow ratio (λ) and the thrust force coefficients (C_T), when the rotor operates at different relative distances to the ground surface (H/R), at different pitching angles (θ). Firstly, the aerodynamic characteristics must be uploaded and properly implemented in the applied computational code. The following aerodynamic characteristics have been defined: lift force coefficient (Cl) vs. the angle of attack (α), drag force coefficient (Cd) vs. the angle of attack (α), airfoil polar Cl (Cd), and the pitching moment coefficient (Cm) vs. angle of attack (α). The initial rotor geometry characteristics, the air parameters, and the finite number of elements, applied in the computational methodology, are represented in the second and third sections of the algorithm, shown in Figure 4. The hovering state is defined through the weight force (W) and the tangential speed in the tip section (V_{tip}) of each blade. Finding the angle of attack distribution along the propeller blade span is essential for calculating the inflow distribution, a major defining parameter in the blade element-momentum analysis. Once the inflow distribution is found, considering all the variable parameters, such as the collective pitch angle (θ), the coefficients of thrust (C_T) can be evaluated for the out-ground effect conditions within the previously defined tolerance range. The calculation of the inflow distribution and consequently the thrust in out-ground effect conditions can be used as a base for making predictions for the in-ground effect zone via applying a proper empirical correction. Hayden and Cheeseman and Bennet empirical models have been applied for correcting the inflow ratio (λ), according to section 2. As a result, once the coefficients are calculated for the whole set of testing conditions, the thrust coefficient (C_T) dependency over the relative distance to ground (H/R) varying the collective pitch angle (θ) can be plotted.

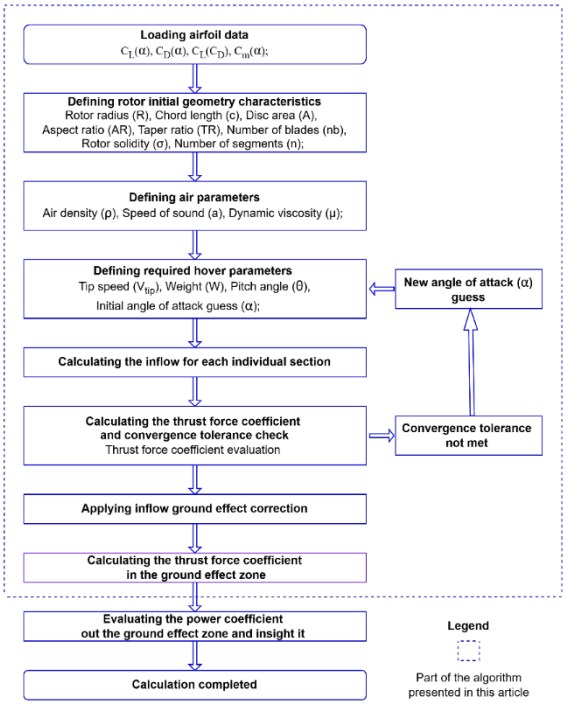

Figure 4. Computational algorithm. Flow diagram

5. Results

The application of the algorithm, presented in Figure 4, allows the velocity filed characterization around the helicopter rotor in terms of inflow ratio distribution (λ) evaluated in the rotational plane. In Table 5, a full inflow ratio (λ) estimation for each individual blade element varying the blade collective pitch angle (θ) is presented for the hovering helicopter in ground effect at a relative distance from the rotational plane to the ground surface $H/R = 1$ and for fixed rotational frequency n = 950 rpm. The thereby presented values clearly indicate the general trend of the inflow ratio (λ) distribution along the blade length for each individual pitch angle (θ): second order curves, reaching their maximums at approximate relative radial distance $r/R = 0.65$. Moreover, an increase in in the blade collective pitch angle (θ) for every constant relative radial distance (r/R), leads to a corresponding increase in the estimated inflow ratio values (λ).

Figure 5 represents the inflow distribution for the hovering rotor in ground effect. All the curves presented in Figure 5 follow smooth trend without any high frequency fluctuations along the blade length. According to the general theory, when the rotor operates at a fixed distance to the ground, an increase in the collective pitch angle (θ) leads to a corresponding increase in the inflow ratio (λ) at each individual blade element. For the smallest relative radial distance r/R = 0.1, the inflow ratio (λ) experiences an increase starting from 0.013 to 0.029 when increasing the blade element angle (θ) from $\theta_1 = 9°$ to $\theta_5 = 21°$. At a relative distance r/R = 0.5, a rise in the inclination angle (θ), from $\theta_1 = 9°$ to $\theta_5 = 21°$, produces a corresponding increase in the inflow ratio (λ) from approximately 0.041 to 0.070, respectively. The largest inflow ratio (λ) increment can be observed at relative radial distance $r/R = 0.9$, when increasing the pitch angle (θ), where (λ) increases from approximately 0.031 at $\theta_1 = 9°$ to 0.068 at $\theta_5 = 21°$. When the helicopter rotor operates with a rotational frequency n = 950 rpm and hovers at a fixed relative distance H/R = 1 with collective pitch angle $\theta_1 = 9°$, the inflow ratio curve (λ) starts rising from 0.013 at r/R = 0.1 up to its maximum equal to 0.042 at approximate relative radial distance r/R = 0.60, then continues with a downward trend

Table 5. Inflow ratio (λ) at each blade element (r/R), varying the collective pitch angle (θ) for rotational frequency n = 950 rpm and $H/R = 1$

Rotational Frequency n = 950 rpm, H/R = 1					
Relative Radial Distance	Inflow Ratio (λ)				
(r/R)	θ_1 = 9°	θ_2 = 12°	θ_3 = 15°	θ_4 = 18°	θ_5 = 21°
0.1	0.013	0.018	0.022	0.025	0.029
0.2	0.025	0.030	0.037	0.041	0.045
0.3	0.032	0.039	0.046	0.052	0.056
0.4	0.039	0.044	0.054	0.060	0.064
0.5	0.041	0.049	0.059	0.066	0.070
0.6	0.042	0.050	0.062	0.069	0.072
0.7	0.040	0.050	0.062	0.070	0.073
0.8	0.036	0.046	0.061	0.069	0.072
0.9	0.031	0.038	0.054	0.065	0.068

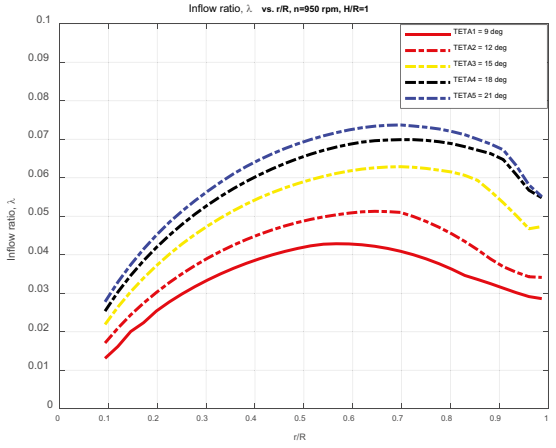

Figure 5. Inflow distribution (λ) vs. the relative blade radius (r/R), varying the collective pitch angle (θ) at H/R = 1 and n = 950 rpm

Table 6. Inflow ratio (λ) at each blade element (r/R), varying the relative distance from the rotor rotational plane to the ground surface (H/R) for blade inclination angle θ_4 = 18° and rotational frequency n = 950 rpm

Rotational Frequency n = 950 rpm, θ_4 = 18°				
Relative Radial Distance	Inflow Ratio (λ)			
(r/R)	H/R = 2	H/R = 1	H/R = 0.5	H/R = 0.25
0.1	0.025	0.021	0.018	0.011
0.2	0.042	0.036	0.029	0.020
0.3	0.053	0.047	0.037	0.025
0.4	0.061	0.053	0.042	0.029
0.5	0.068	0.059	0.046	0.031
0.6	0.070	0.061	0.048	0.033
0.7	0.071	0.062	0.049	0.033
0.8	0.070	0.060	0.048	0.033
0.9	0.062	0.053	0.043	0.029

reaching the value of 0.031 at relative radial distance r/R = 0.9. In addition, the inflow ratio curves (λ), for the collective pitch angle θ_5 = 21° experience an increase, starting from 0.029 for relative radial distance r/R = 0.1 and soaring up to 0.073 at relative radial distance r/R = 0.7, the highest value quantified in this study.

In Table 6 the inflow distribution values (λ) for the whole set of relative distances (H/R), fixed rotational frequency n = 950 rpm and collective pitch angle θ_4 = 18° are presented. According to the data shown in Table 6, a decrease in the relative distances to the ground (H/R) leads to a corresponding decline in the inflow ratio (λ) values for every fixed radial coordinate (r/R). For the given collective pitch angle θ_4 = 18° and rotational frequency n = 950 rpm, for all the studied cases, the inflow curves follow a second order curve path, starting from the rotor hub (r/R = 0.1) up to the tip sections (r/R = 0.9). This trend remains valid for all the relative distances (H/R).

In addition to the values presented in Table 6, graphical representation can be further derived. Figure 6 presents the correlation between the inflow distribution (λ) over the relative blade radius (r/R), varying the relative distance to ground (H/R) at fixed collective pitch angle θ_4 = 18° and rotational frequency n = 950 rpm. The inflow distribution curves experience a decrease for every single coordinate in spanwise direction once the distance to the ground surface at which the helicopter rotor operates decreases. The inflow ratio value (λ) in the root section (r/R = 0.1) follows an upward trend, starting from 0.018 up to 0.025, when the operational distance increases from H/R = 0.5 to H/R = 2. The largest increase in the inflow rate is observed in the blade element located in relative radial distance r/R = 0.7, where an increase in the operational distance from H/R = 0.5 to H/R = 2 leads to a rise in inflow ratio (λ) from 0.049 up to 0.071, respectively. The inflow distribution curve, derived for the relative operational distance H/R = 0.5 follows a parabolic trend starting from approximately 0.018, then reaching its maximum equal to 0.049 at relative radial distance H/R = 0.7, and further decreases

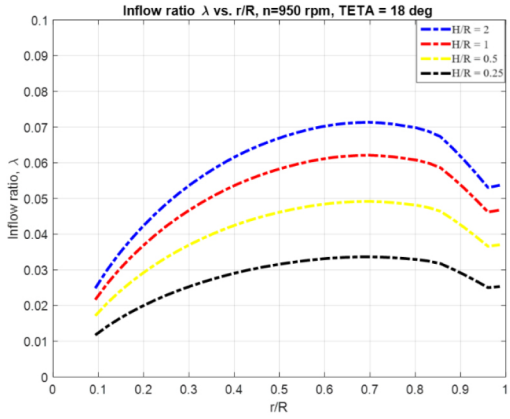

Figure 6. Inflow distribution (λ) vs. the relative blade radius (r/R), varying the relative distance (H/R) for θ_4 = 18° and n = 950 rpm

to 0.043 at relative radial coordinates r/R = 0.9. When the helicopter rotor operates at a collective pitch angle θ_4 = 18° with rotational frequency n = 950 rpm, the inflow ratio (λ) increases from approximately 0.04 to 0.06, when increasing the relative distance from H/R = 0.5 to H/R = 2 at relative radial distance r/R = 0.9.

The inflow distribution curve at relative distance H/R = 2 at fixed rotational frequency n = 950 rpm and collective pitch angle θ = 18° represents the highest inflow ratio values, quantified during this study, starting from approximately 0.025 at r/R = 0.1, reaching its maximum of 0.071 at r/R = 0.7, then declining to 0.062 at relative distance r/R = 0.9.

The reduction in the inflow ratio, when decreasing the relative distance to the ground at constant collective pitch angle (θ) will lead to a corresponding rise in the amount of generated thrust (T), a decrease in the required power, and will cause the same effect on their coefficients (C_T) and (C_P), respectively.

The inflow ratio (λ) quantification along the blade span can be directly applied to the thrust (C_T) and power coefficients (C_P) estimation in the ground effect zone. Table 7 illustrates the values of the weighted thrust force coefficients (C_T/σ) along the blade length, obtained for all the tested cases. Moreover, Table 7 represents a comparison between the experimentally evaluated and the numerically derived values for every constant collective pitch angle (θ).

In Figure 7 the normalized thrust force coefficient (C_T/σ) dependency over the collective pitch angle (θ), varying the relative distance to the ground surface (H/R) is presented. The evaluated dependency is a corner one for the performed analysis and the first step towards the rotor performance characterization.

The closer to the ground the helicopter rotor operates, the higher inflow ratio (λ) decrease is observed, which directly leads to an increase in the generated thrust (T). For every constant relative distance from the helicopter rotor to the ground surface (H/R) an increase in the collective pitch angle (θ) leads to a corresponding rise in the magnitude of both the experimentally derived and the numerically calculated weighted thrust force coefficients (C_T/σ). In the ground effect zone, when the helicopter rotor operates at relative distance to the ground H/R = 0.5, the calculated weighted thrust force coefficient (C_T/σ) follows an upward trend starting from 0.065 for the collective pitch angle θ_1 = 9°, rising to the value of 0.113 at θ_3 = 15°, then reaching the maximum equal to 0.141 at collective pitch angle θ_5 = 21°. The predicted values for the hovering helicopter rotor out ground effect conditions (H/R = 2) start rising from 0.045 at θ_1 = 9° up to 0.110 at θ_5 = 21°.When the helicopter rotor operates at collective pitch angle θ_2 = 12°, an increase in the operational distance to the ground surface from 0.5 R to 2 R leads to a decline in the calculated weighted thrust force coefficient values (C_T/σ) from 0.08 to 0.06. The experimentally derived weighted thrust force coefficient values (C_T/σ) at θ_2 = 12°, when increasing the operational distance to the ground surface from 0.5 R to 2 R amount to 0.083 and 0.059, respectively. According to the derived results, it can be concluded that the numerical predictions for the

Table 7. Experimental and numerical weighted thrust force coefficients $\left(C_T/\sigma\right)$, varying the collective pitch angle (θ) and the relative distance (H/R)

Weighted Thrust Force Coefficient (C_T/σ)										
	EXPT	BEMT	EXPT	BEMT	EXPT	BEMT	EXPT	BEMT	EXPT	BEMT
	θ_1 = 9°		θ_2 = 12°		θ_3 = 15°		θ_4 = 18°		θ_5 = 21°	
H/R = 2	0.032	0.045	0.059	0.060	0.083	0.084	0.102	0.103	0.109	0.110
H/R = 1	0.041	0.051	0.072	0.069	0.101	0.097	0.120	0.115	0.125	0.122
H/R = 0.5	0.059	0.065	0.083	0.080	0.115	0.113	0.132	0.131	0.138	0.141
H/R = 0.25	0.070	0.083	0.097	0.105	0.120	0.142	0.125	0.164	0.134	0.178

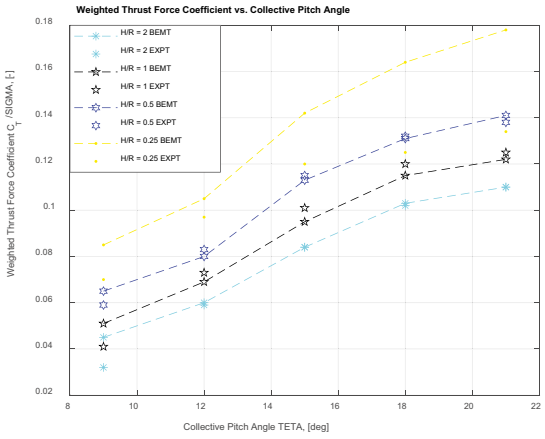

Figure 7. Weighted thrust force coefficients (C_T/σ) vs. collective pitch angle (θ), varying the relative distance (H/R)

weighted thrust force coefficients (C_T/σ) vs. the collective pitch angle (θ) show considerably good agreement to the experimental data in the range of up to 5% for collective pitch angles θ > 9°. A deviation is observed in the extreme ground effect conditions, specifically in the curve, which represents the normalized thrust force coefficient (C_T/σ), when the helicopter rotor operates at 0.25 R distance to the surface. The main reason for this deviation is the inability of the applied empirical models to predict accurately the flow parameters, when the helicopter rotor operates extremely close to the ground surface.

Experimentally derived results for the weighted coefficients of thrust (C_T/σ), estimated when the helicopter rotor operates at relative distance to the ground surface $H/R = 0.25$ for high collective pitch angles θ_4 = 18° to θ_5 = 21° experience a decrease in comparison with the coefficients evaluated for $H/R = 0.5$ due to stall in extreme ground effect conditions.

6. Conclusions

This research paper presents the preliminary results, obtained throughout the conducted study, which aims to apply coupled empirical – blade element – momentum mathematical model for making helicopter rotor performance predictions in ground effect. Proposed coupling between the blade element and the momentum theory combined with empirical corrections provides an estimation of the helicopter rotor inflow ratio (λ) in the rotational plane, when varying several parameters such as the collective pitch angle (θ) and the relative distance from the helicopter rotor rotational plane to the ground surface (H/R). The followed methodology presents the estimation of the inflow ratio (λ) and the weighted thrust force coefficients (C_T/σ), firstly, for the out-ground effect conditions, following an empirical correction regarding the inflow ratio (λ) values in the ground effect zone. The proposed coupling clearly quantified the inflow ratio (λ) distribution and the weighted thrust force coefficients (C_T/σ) values in the ground effect zone, except for the results in extreme ground effect. The characterization of these values in the ground effect zone is crucially essential for designing automatic flight control systems and properly controlling the rotorcraft in such conditions. Quantification of the produced thrust (*T*) in ground effect conditions and then mathematically estimating its values depending on several parameters provides an evaluation of the helicopter rotor performance during lifting off and landing. Dependencies between the inflow ratio (λ) along the blade relative radius (r/R) at a constant relative distance to the ground (H/R), varying the collective pitch angle (θ) and vice versa, are derived. Inflow distribution curves follow smooth second order curve path, starting from the helicopter rotor hub elements up to the tip sections and do not experience any abrupt changes. The maximum inflow ratio distribution (λ) for a fixed relative distance from the rotational plane to the ground surface (H/R) is observed at approximate radial coordinate r/R = 0.7. In general, an increase in the collective pitch angle (θ) at a constant relative distance to the ground (H/R) leads to a rise in the inflow ratio (λ). The increase in the inflow distribution values (λ), when increasing the collective pitch angle (θ) leads to a consequent rise in the calculated weighted thrust force coefficients (C_T/σ). Finally, a dependency between the weighted thrust force coefficient (C_T/σ) vs. the collective pitch angle (θ) is drawn. For every constant relative distance from the helicopter rotational plane to the ground surface (H/R), an increase in the collective pitch angle (θ) leads to an increase in the calculated weighted thrust force coefficient (C_T/σ). For every constant collective pitch angle (θ), a reduction in the relative distance to the ground (H/R) provides a direct increase in the weighted thrust force coefficients. All the mathematically derived results show good agreement with the previously obtained experimental, except for the curve at 0.25 *R*, due to the inability of the applied empirical models to predict correctly in the extreme ground effect zone. Future work will include a full characterization of the aerodynamics characteristics in ground effect conditions.

Acknowledgements

This research is conducted with the support of the Bulgarian – American Commission for Educational Exchange Fulbright within a collaboration with the University of Maryland in College Park.

Author contributions

The author contributing to this research is fully responsible for the application of the proposed algorithm and the consequent analysis of the derived results.

Disclosure statement

The author declares to have no known competing financial, professional or personal interests from other parties that could influence the research presented in this paper.

References

Bohorquez, F., Samuel, P., Sirohi, J., Pines, D., & Rudd, L. (2023). Design, analysis and hover performance of a rotary wing micro air vehicle. *Journal of The American Helicopter Society*, *48*(2), 80–90. https://doi.org/10.4050/JAHS.48.80

Brown, R., & Whitehouse, G. (2004). Modelling rotor wakes in ground effect. *Journal of American Helicopter Society*, *49*(3), 238–249. https://doi.org/10.4050/JAHS.49.238

Conyers, S., Rutherford, M., & Valavanis, K. (2018). An empirical evaluation of ground effect for small-scale rotorcraft. In 2018 *IEEE International Conference on Robotics and Automation* (*ICRA*). IEEE. https://doi.org/10.1109/ICUAS.2018.8453469

Eberhart, G., & Wilhelm, J. (2018). Development of a ground effect bemt analysis method for multirotor sUAS. In *AIAA Information Systems-AIAA Infotech*. Aerospace Research Central. https://doi.org/10.2514/6.2018-0747

Fradenburgh, E. (1960). The helicopter and the ground effect machine. *Journal of the American Helicopter Society*, *5*(4), 24–33(10). https://doi.org/10.4050/JAHS.5.4.24

Georgiev, G., Panayotov, F., Serbezov, V., & Todorov, M. (2024). Experimental study of static characteristics of a helicopter rotor in ground effect. *AIP Conference Proceedings*, *2980*(1), Article 050002. https://doi.org/10.1063/5.0186410

Georgiev, G., Serbezov, V., & Todorov, M. (2022). Experimental study of multicopter propeller performance near the ground at different inclination angles. *AIP Conference Proceedings*, *2557*, Article 020002. https://doi.org/10.1063/5.0106920

Gilad, M., Chopra, I., & Rand, O. (2011). Performance evaluation of a flexible rotor in extreme ground effect. In *37th European Rotorcraft Forum* (pp. 1–10). Italy, Milan.

Graber, A., Rosen, A., & Seginer, A. (1991). An investigation of a hovering rotor in ground effect. *The Aeronautical Journal*, *95*(945), 161–169. https://doi.org/10.1017/S0001924000023812

Griffiths, D., Ananthan, S., & Leishman, G. (2005). Predictions of rotor performance in ground effect using a free-vortex wake model. *Journal of the American Helicopter Society*, *50*(4), 302–314(13). https://doi.org/10.4050/1.3092867

Hanker, E., & Smith, R. (1985). Parameters affecting helicopter interactional aerodynamics in ground effect. *Journal of the American Helicopter Society*, *30*(1), 52–61(10). https://doi.org/10.4050/JAHS.30.52

Johnson, W. (2019). *NASA design and analysis of rotorcraft* (Release 1.14). NASA. Ames Research Center.

Johnson, W. (2013). *Rotorcraft aeromechanics*. Cambridge University Press. https://doi.org/10.1017/CBO9781139235655

Khromov, V., & Rand, O. (2008). Ground effect modelling for rotary – wing simulation. In *26th International Congress of the Aeronautical Sciences* (pp. 1–10). Anchorage.

Knight, M., & Hefner, R. (1941). *Analysis of ground effect on lifting airscrew* (National Advisory Committee of Aeronautics Technical Notes №835). UNT Digital Library.

Koning, W., Johnson, W., & Grip, H. F. (2019). Improved Mars helicopter aerodynamic rotor model for comprehensive analyses. *AIAA Journal*, *57*(9). https://doi.org/10.2514/1.J058045

Kutz, B., Großmann, T., Keßler, M., & Krämer, E. (2013). Experimental and numerical examination of a helicopter hovering in ground effect. *CEAS Aeronautical Journal*, *4*, 397–408. https://doi.org/10.1007/s13272-013-0084-x

Leishman, G. (2006). *Principles of helicopter aerodynamics* (2nd ed.). Cambridge University Press.

Lighthill, J. (1979). A simple fluid-flow model of ground effect on hovering. *Journal of Fluid Mechanics*, *93*(4), 781–797. https://doi.org/10.1017/S0022112079002032

Madsen, H., Mikkelsen, R., Øye, S., Bak, S., & Johansen, J. (2007). A detailed investigation of the blade element momentum (BEM) model based on analytical and numerical results and proposal for modifications of the BEM model. *Journal of Physics: Conference Series*, *75*(1), Article 012016. https://doi.org/10.1088/1742-6596/75/1/012016

Nagaraj, V., Chopra, I., & Pines, D. (2021). *Gamera: A human powered helicopter – in pursuit of an aviation milestone*. American Institute of Aeronautics and Astronautics. https://doi.org/10.2514/4.106217

Nathan, N., & Green, R. (2011). The flow around a model helicopter main rotor in ground effect. *Experiments in Fluids*, *52*, 151–166. https://doi.org/10.1007/s00348-011-1212-1

Pulla, D., & Conlisk, A. (2007). A lifting surface study of helicopter aerodynamics in ground effect. In *45th AIAA Aerospace Science Meeting and Exhibit* (pp. 1–15). ARC. https://doi.org/10.2514/6.2007-1279

Purvis, R. (2002). *Rotor blades and ground effect* [Doctoral dissertation, University College London]. UCL Discovery.

Rotaru, C., & Todorov, M. (2017). *Helicopter flight physics*. Intech Open. https://doi.org/10.5772/intechopen.71516

Todorov, M., Dobrev, I., Massouh, F., & Velkova C. (2012). An investigation of the motion of a rotor with flapping and LEAD/LAG hinges in hover. *BulTrans – 2012 Proceedings*. ResearchGate.

Zhao, J., & He, C. (2015). Physics-based modeling of viscous ground effect for rotorcraft applications. *Journal of the American Helicopter Society*, *60*(3), 1–13(13). https://doi.org/10.4050/JAHS.60.032006